

Estimation of the stiffness tensor of dry rock through numerical simulations based on rock physics

Juan E. Santos * School of Earth Sciences and Engineering, Hohai University, Universidad de Buenos Aires, Facultad de Ingeniería, Instituto del Gas y del Petróleo, Department of Mathematics, Purdue University, A. Sanchez Camus, Facultad de Ciencias Astronómicas y Geofísicas, Universidad Nacional de La Plata, Gabriela B. Savioli, Universidad de Buenos Aires, Facultad de Ingeniería, Instituto del Gas y del Petróleo, Patricia M. Gauzellino, Facultad de Ciencias Astronómicas y Geofísicas, Universidad Nacional de La Plata, Jing Ba, School of Earth Sciences and Engineering, Hohai University

SUMMARY

From a mechanical perspective, organic mudrocks are viscoelastic media whose anisotropy can be accurately represented using a vertical transverse isotropy (VTI) model. These reservoirs exhibit ultra-low permeability, typically in the range of nano to microdarcies, and possess a complex pore structure. Such characteristics, along with the influence of capillary forces and the relative permeabilities of saturating fluids, significantly impact the hydraulic properties and mechanical behavior of the reservoir during production. This study introduces a practical methodology to estimate the stiffness tensor of dry rock through numerical simulations based on rock physics, incorporating mechanical, mineralogical, and petrophysical data from a core extracted from the lower section of the Vaca Muerta Formation, located in the Neuquén Basin, Argentina. After determining the dry-rock stiffness tensor, the proposed method enables the simulation of different fluid saturation conditions and seismic source frequencies, ranging from laboratory experiments and well logging to field seismic studies. Numerical results exhibit excellent agreement with laboratory data, with errors below 5 %, validating the proposed methodology as an effective tool for evaluating critical phenomena such as attenuation and dispersion caused by wave-induced fluid flow (WIFF). Once the model parameters have been calibrated, the stiffness tensor can be extrapolated to other areas within the block using only mineralogical and petrophysical information (porosity and permeability). This significantly simplifies the geomechanical and seismic characterization of unconventional reservoirs.

INTRODUCTION

One of the important mechanisms of seismic attenuation in fluid-saturated porous media is wave-induced fluid flow, by which the fast compressional wave is converted to slow (diffusive) Biot waves at mesoscopic-scale heterogeneities, which are larger than the pore size but much smaller than the predominant wavelengths of the fast compressional and shear waves (Carcione et al, 2007)

MESOSCOPIC-FLOW ATTENUATION THEORY FOR VTI MEDIA

The Vaca Muerta formation is characterized by a transversely isotropic anisotropy with a vertical axis - VTI (?), although it may change its elastic symmetry due to the presence of frac-

tures. Let us consider x_1 and x_3 as the horizontal and vertical coordinates, respectively. A VTI medium is characterized by five independent elastic moduli $c_{11}, c_{13}, c_{33}, c_{55}, c_{66}$. In this case, the stress-strain relationship in Voigt notation is given by (Tsvankin et al, 2001).

$$\begin{bmatrix} \sigma_{11} \\ \sigma_{22} \\ \sigma_{33} \\ \sigma_{23} \\ \sigma_{31} \\ \sigma_{12} \end{bmatrix} = \begin{bmatrix} c_{11} & c_{12} & c_{13} & 0 & 0 & 0 \\ c_{12} & c_{11} & c_{13} & 0 & 0 & 0 \\ c_{13} & c_{13} & c_{33} & 0 & 0 & 0 \\ 0 & 0 & 0 & c_{55} & 0 & 0 \\ 0 & 0 & 0 & 0 & c_{55} & 0 \\ 0 & 0 & 0 & 0 & 0 & c_{66} \end{bmatrix} \cdot \begin{bmatrix} \epsilon_{11} \\ \epsilon_{22} \\ \epsilon_{33} \\ 2\epsilon_{23} \\ 2\epsilon_{31} \\ 2\epsilon_{12} \end{bmatrix} \quad (1)$$

with the vectors σ and ϵ being the stress and the strain, respectively, and $c_{12} = c_{11} - 2c_{66}$

The attenuation of the material is considered through an equivalent viscoelastic medium, characterized by complex and frequency dependent stiffness p_{ij} , where the imaginary part represents the attenuation. Therefore, if $\tilde{\sigma}$ and $\tilde{\epsilon}$ denote the stress and strain of the equivalent viscoelastic TVI medium:

$$\begin{bmatrix} \tilde{\sigma}_{11} \\ \tilde{\sigma}_{22} \\ \tilde{\sigma}_{33} \\ \tilde{\sigma}_{23} \\ \tilde{\sigma}_{31} \\ \tilde{\sigma}_{12} \end{bmatrix} = \begin{bmatrix} p_{11} & p_{12} & p_{13} & 0 & 0 & 0 \\ p_{12} & p_{11} & p_{13} & 0 & 0 & 0 \\ p_{13} & p_{13} & p_{33} & 0 & 0 & 0 \\ 0 & 0 & 0 & p_{55} & 0 & 0 \\ 0 & 0 & 0 & 0 & p_{55} & 0 \\ 0 & 0 & 0 & 0 & 0 & p_{66} \end{bmatrix} \cdot \begin{bmatrix} \tilde{\epsilon}_{11} \\ \tilde{\epsilon}_{22} \\ \tilde{\epsilon}_{33} \\ 2\tilde{\epsilon}_{23} \\ 2\tilde{\epsilon}_{31} \\ 2\tilde{\epsilon}_{12} \end{bmatrix} \quad (2)$$

with $p_{12} = p_{11} - 2p_{66}$

White et al (1975) described the equivalent viscoelastic medium of two alternating thin layers of thickness d_1 and d_2 , with symmetry axes orthogonal to the layering plane. Their theory gives the complex and frequency dependent stiffness p_{33} , as:

$$p_{33} = \left[\frac{1}{c_{33}} + \frac{2(r_2 - r_1)^2}{i\omega(d_1 + d_2)(I_1 + I_2)} \right]^{-1}, \quad (3)$$

where

$$r = \frac{\alpha M}{E_G}, I = \frac{\eta}{\kappa a} \coth\left(\frac{ad}{2}\right), a = \sqrt{\frac{i\omega\eta E_G}{\kappa M E_m}} \quad (4)$$

for each single layer. In Eq.(4), $\alpha = 1 - \frac{K_m}{K_s}$, $E_G = E_m + \alpha^2 M$,

$E_m = K_m + \frac{4}{3}\mu$, $M = \left[\frac{\alpha - \phi}{K_s} + \frac{\phi}{K_f} \right]^{-1}$, with K_s , K_m and K_f the solid grains, dry matrix and saturant fluid bulk moduli; μ is the shear modulus, η is the fluid viscosity, κ is the permeability, ω the frequency and i the imaginary unit.

Estimation of the stiffness tensor of dry rock through numerical simulations based on rock physics

White model has been generalized by Krzikalla and Müller (2011) to anisotropic media, i.e., they computed p_{33} as in Eq.(3) and obtained the other five stiffnesses of the equivalent TIV medium as,

$$p_{ij}(\omega) = c_{ij} + \left(\frac{c_{ij} - c_{ij}^r}{c_{33} - c_{33}^r} \right) [p_{33}(\omega) - c_{33}], \quad (5)$$

where c_{ij}^r are the relaxed stiffnesses, computed as shown in the Appendix (Gelinsky and Shapiro, 1997). The main assumption in Eq. (5) is that the fluid-flow direction is orthogonal to the layering and that the relaxation behavior is described by a single stiffness, $p_{33}(\omega)$ (Krzikalla and Müller, 2011). Thus the theory is valid for plane layers and can not be used when 2D or 3D heterogeneities are present.

Finally, the velocity and quality factor of the qP, qS and SH waves for the equivalent anisotropic medium are computed from the complex velocities, as it may be seen in (Carcione, 2007).

RESULTS

Data

A core from the Vaca Muerta Formation is the source of the measured data, which consist of rock mineralogy and phase velocities, vp_{11} , vp_{33} , vp_{55} and vp_{66} of the dry core.

The objective of this study is to verify that by knowing the mineralogy and applying a numerical physics of rock experiment, we are able to accurately estimate the elastic tensor coefficients p_{ij} . The numerical experiment considers a domain of size 1 mm, divided in 80 layers, 79 layers of Material 1 and 1 layer of Material 2. Material 1 is composed of 7 minerals, including 23 % Kerogen, 37.27 % Clay, 14.61 % Quartz, 10.68 % Calcite, 2.57 % Plagioclase, 2.37 % Dolomite and 3.5 % Pyrite. Using the solid grains bulk and shear moduli of each mineral and a generalized Krief model (Carcione et al, 2005), we obtained the values K_s , K_m , μ_m as shown in Table 1. We also computed the average density of Material 1

Besides, we have 1 layer of Material 2 consisting of Kerogen. Its properties can be seen in Table 1. Both materials have 6 % porosity and $2.75 \times 10^{-18} \text{ m}^2$ permeability.

Table 1. Properties of Materials

Property	Material 1 (Composite)	Material 2 (Kerogen)
K_s (GPa)	34.34	7.0
K_m (GPa)	29.19	1.29
μ_m (GPa)	15.69	0.36
ρ (kg/m^3)	2487	1400

Computed VTI phase velocities using the dry-core data

We compute the numerical stiffness coefficients p_{ij} applying the methodology described in section "Mesoscopic-flow attenuation theory for VTI media" and the data of Table 1. We consider a 1 mm thickness square sample with only one period. The mesh size is 1.25×10^{-5} , then the sizes of layers 1 and 2 are 9.875×10^{-4} and 1.25×10^{-5} . Since the phase velocity

data come from a dry sample, in the numerical experiment we consider the saturating fluid to be air. Table 2 summarizes the results of the VTI experiments.

Table 2. Phase velocities from the numerical experiments and the measured ones, error percentage. Frequency is 1 MHz

Phase velocity vp (m/s)	Computed	Measured	Percentage error
vp_{11}	4538.29	4331	4.79 %
vp_{33}	4008.93	4217.47	4.96 %
vp_{55}	2098.69	2193.61	4.33 %
vp_{66}	2581.97	2464	4.79 %

At all velocities, an error of less than 5% is obtained, which is considered a very good match since it is within the range of measurement errors. We can then rely on the numerically estimated values of the stiffness coefficients p_{ij} , which are shown in Table 3.

Table 3. Numerical p_{ij} values from the VTI experiments. Frequency is 1 MHz

p_{11}
(47881607223.002250, 34039.066160)
p_{33}
(37362983980.381652, 223305.323451)
p_{55}
(10239564921.821903, 0.0)
p_{66}
(10239564921.827581, 0.0)
p_{13}
(13930827662.989664, 10086.232336)

Figure 1 shows the polar representation of phase velocities of qP, qSV and SH waves at 1 MHz. Anisotropy is clearly observed, mainly in the behavior of velocities of qP and SH waves.

Phase velocities and attenuation using hydrocarbon saturated samples

In this subsection the same sample of the previous experiment is considered, but with the two layers saturated by 100 % oil. '11' and '33' waves phase velocities as function of frequency are shown in Figures 2 and 3, respectively. The corresponding attenuation factors $1000/Q_{11}$ and $1000/Q_{33}$ are displayed in Figures 4 and 5.

Note that the attenuation peak for '33' waves is shifted to higher frequencies as compared with '11' waves. This is also observed in Santos et al (2019).

Estimation of the stiffness tensor of dry rock through numerical simulations based on rock physics

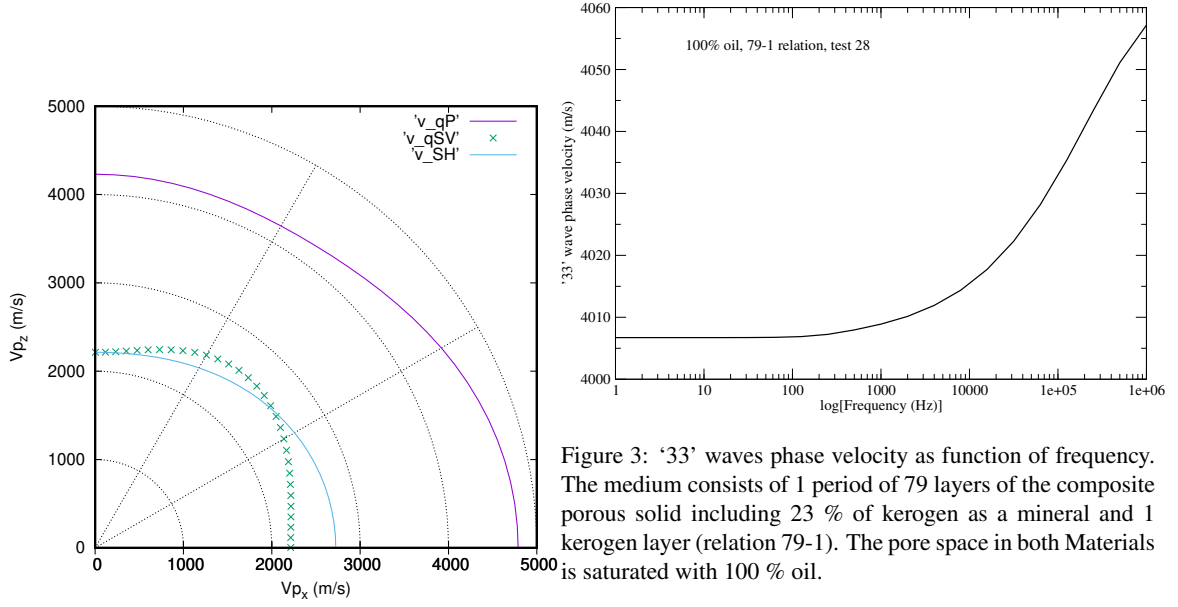


Figure 1: Polar representation of phase velocities of qP, qSV and SH waves at 1 MHz. The medium consists of 1 period of 79 dry layers of the composite porous solid including kerogen as a mineral with 23 % proportion, and 1 dry kerogen layer (relation 79-1).

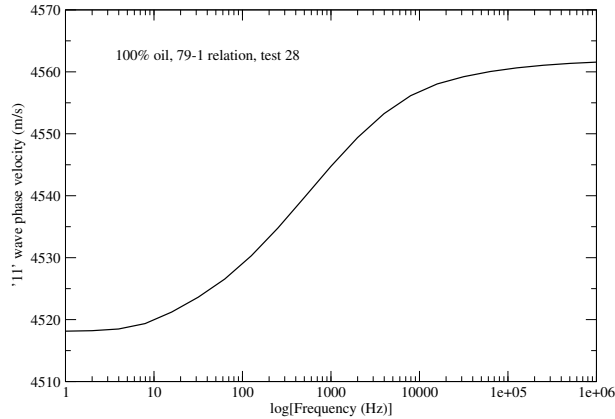


Figure 2: '11' waves phase velocity as function of frequency. The medium consists of 1 period of 79 layers of the composite porous solid including 23 % of kerogen as a mineral and 1 kerogen layer (relation 79-1). The pore space in both Materials is saturated with 100 % oil.

APPENDIX A

$$\begin{aligned}
 c_{66}^r &= \langle \mu \rangle, \\
 c_{11}^r - 2c_{66}^r &= c_{12}^r = 2 \left\langle \frac{\lambda_m \mu}{E_m} \right\rangle + \left\langle \frac{\lambda_m}{E_m} \right\rangle^2 \left\langle \frac{1}{E_m} \right\rangle^{-1} \\
 &\quad + \frac{B_6^{*2}}{B_8^*}, \\
 c_{13}^r &= \left\langle \frac{\lambda_m}{E_m} \right\rangle \left\langle \frac{1}{E_m} \right\rangle^{-1} + \frac{B_6^* B_7^*}{B_8^*}, \\
 c_{33}^r &= \left[\left\langle \frac{1}{E_m} \right\rangle - \left\langle \frac{\alpha}{E_m} \right\rangle^2 \left\langle \frac{E_G}{ME_m} \right\rangle^{-1} \right]^{-1}, \\
 c_{55}^r &= \langle \mu^{-1} \rangle^{-1}, \\
 B_6^* &= -B_8^* \left(2 \left\langle \frac{\alpha \mu}{E_m} \right\rangle + \left\langle \frac{\alpha}{E_m} \right\rangle \left\langle \frac{\lambda_m}{E_m} \right\rangle \left\langle \frac{1}{E_m} \right\rangle^{-1} \right), \\
 B_7^* &= -B_8^* \left\langle \frac{\alpha}{E_m} \right\rangle \left\langle \frac{1}{E_m} \right\rangle^{-1}, \\
 B_8^* &= \left[\left\langle \frac{1}{M} \right\rangle + \left\langle \frac{\alpha^2}{E_m} \right\rangle - \left\langle \frac{\alpha}{E_m} \right\rangle^2 \left\langle \frac{1}{E_m} \right\rangle^{-1} \right]^{-1},
 \end{aligned} \tag{A-1}$$

where $\langle \cdot \rangle$ means weighted average between layers.

When there is no interlayer flow (unrelaxed regime), the coef-

Estimation of the stiffness tensor of dry rock through numerical simulations based on rock physics

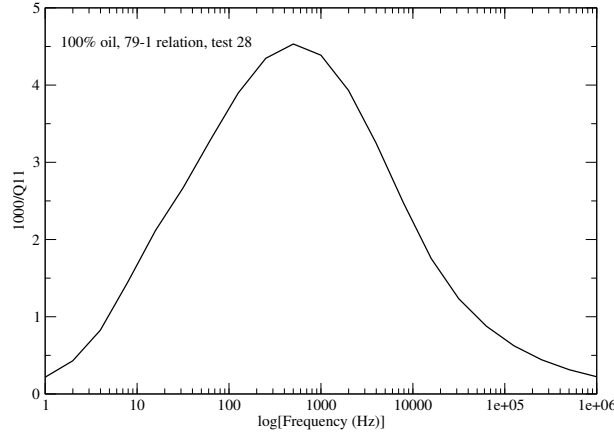


Figure 4: ‘11’ waves attenuation factor 1000/Q11 as function of frequency. The medium consists of 1 period of 79 layers of the composite porous solid including 23 % of kerogen as a mineral and 1 kerogen layer (relation 79-1). The pore space in both Materials is saturated with 100 % oil.

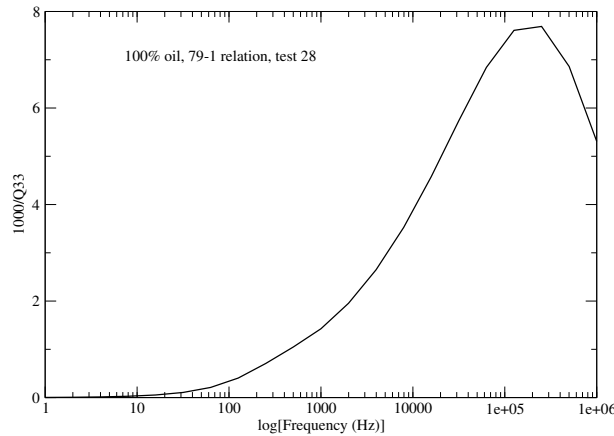


Figure 5: ‘33’ waves attenuation factor 1000/Q33 as function of frequency. The medium consists of 1 period of 79 layers of the composite porous solid including 23 % of kerogen as a mineral and 1 kerogen layer (relation 79-1). The pore space in both Materials is saturated with 100 % oil

ficients are (Gelinsky and Shapiro, 1997),

$$\begin{aligned} c_{66} &= c_{66}^r, \\ c_{11} - 2c_{66} &= c_{12} = 2 \left\langle \frac{(E_G - 2\mu)\mu}{E_G} \right\rangle + \left\langle \frac{E_G - 2\mu}{E_G} \right\rangle^2 \left\langle \frac{1}{E_G} \right\rangle^{-1}, \\ c_{13} &= \left\langle \frac{E_G - 2\mu}{E_G} \right\rangle \left\langle \frac{1}{E_G} \right\rangle^{-1}, \\ c_{33} &= \left\langle \frac{1}{E_G} \right\rangle^{-1}, \\ c_{55} &= c_{55}^r. \end{aligned} \quad (A-2)$$

REFERENCES

- J. M. Carcione and S. Picotti, P-wave seismic attenuation by slow-wave diffusion, Effects of inhomogeneous rock properties, *Geophysics* 71 (2006) O1-O8.
- Jose M. Carcione, Hans B. Helle, Juan E. Santos and Claudia L. Ravazzoli, A constitutive equation and generalized Gassmann modulus for multimineral porous media, *Geophysics*,70 (2); doi: 10.1190/1.1897035
- S. Gelinsky and S. A. Shapiro, Poroelastic Backus-averaging for anisotropic, layered fluid and gas saturated sediments, *Geophysics* 62 (1997) 1867-1878.
- González Celis, R. et al. (2020) Matriz energética mundial y el cambio climático: Estado actual. *Master Thesis - Gestión Sostenible de la Energía*.
- Grechka, V. and Tsvankin, I. (2003) Feasibility of seismic characterization of multiple fracture sets. *Geophysics*, **68**, 1399–1407.
- F. Krzikalla and T. M. Müller, Anisotropic P-SV-wave dispersion and attenuation due to interlayer flow in thinly layered porous rocks, *Geophysics* 76 W 135 (2011); doi:10.1190/1.3555077.
- J.E. Santos, G.B. Savioli, J. M. Carcione and J. Ba, Effect of capillarity and relative permeability on Q anisotropy of hydrocarbon source rocks, *Geophys. J. Int.* (2019) 218, 1199–1209, doi: 10.1093/gji/ggz217.
- J. E. White, N. G. Mikhaylova and F. M. Lyakhovitskiy, Low-frequency seismic waves in fluid saturated layered rocks, *Physics of the Solid Earth* 11 (1975) 654-659.